*Inorg. Chem.* **2009**, *48*, 4021−4030


# Long-Range Through-Bond Heteronuclear Communication in Platinum Complexes

**Olena V. Zenkina,[†] Leonid E. Konstantinovski,[‡] Linda J. W. Shimon,[‡] Yael Diskin-Posner,[‡] Mark A. Iron,[‡] and Milko E. van der Boom*[,†]**

*Departments of Organic Chemistry and Chemical Research Support, The Weizmann Institute of Science, 76100 Rehovot, Israel*

Received October 13, 2008

Four analogous platinum stilbene- and stilbazole-based complexes exhibit unusual long-range heteronuclear spin−spin coupling in solution. Single crystal analysis and NMR experiments show that the $^{19}F$, $^{31}P$, and $^{195}Pt$ nuclei communicate over large distances (0.9−1.3 nm) through bond rather than through space. Spin−spin couplings between $^{195}Pt$ and $^{19}F$ over seven bonds and between $^{31}P$ and $^{19}F$ over eight bonds are observed with $^{7}J_{PtF} = 2.9$ Hz and $^{8}J_{PF} = 11.8$ Hz. Remarkably, a very large spin coupling between $^{195}Pt$ and $^{19}F$ over six bonds ($^{6}J_{PtF} = 40.1$ Hz) is also observed in a structurally related pyridinium complex. Experimental and gNMR (version 5.0) simulated $^{19}F\{^{1}H\}$, $^{31}P\{^{1}H\}$, and $^{195}Pt\{^{1}H\}$ spectra of the complexes reveal a three-spin AMY system (A = $^{31}P$, M = $^{31}P$, Y = $^{19}F$) or a five-spin $AMY_3$ flanked by a four-spin AMXY or a six-spin $AMXY_3$ system (X = $^{195}Pt$), respectively. Density functional theory calculations at the PBE0/SDD level of theory show a $\pi$-conjugated metal−ligand network, which may contribute to the experimentally observed spin−spin interactions.

## Introduction

Heteronuclear NMR-active molecular systems that exhibit large spin−spin coupling across a large number of bonds and distances are potential candidates for molecular-based NMR quantum computing.[1−4] These systems use nuclear spins as quantum bits or "qubits" that communicate via spin−spin coupling.[5−7] Despite the tremendous progress in molecular design, relatively few systems have been shown to exhibit large long-range through-bond nuclear spin−spin coupling.[8−13] Experimental observations of long-range indirect nuclear spin−spin coupling constants are relatively rare because the coupling constants usually are very small or not observed. Theoretical studies show that long-range through-bond interactions are facilitated by $\pi$-conjugation.[5,14−17] Coupled homo- and heteronuclear spins can also be through-space interactions resulting from spatial proximity.[18] For example, compounds **I**−**III** (Chart 1) exhibit long-range homonuclear through-space (**I, III**)[8] or through-bond (**II**)[10,11,17] $^{19}F-^{19}F$ spin couplings. Compound **IV** shows a long-range through-bond $^{31}P-^{1}H$ spin coupling.[12] Hennig et al. recently reported on long-range through-bond $^{1}H-^{19}F$ spin coupling in 5-fluoropyrimidine-substituted RNA.[13]

Complexes **V**−**VII** (Chart 2) are examples of platinum complexes containing heteronuclear spin systems.[19−21] Through space $^{195}Pt-^{19}F$ coupling is observed in complex

* To whom correspondence should be addressed. E-mail: milko.vanderboom@weizmann.ac.il.
[†] Department of Organic Chemistry.
[‡] Department of Chemical Research Support.

(1) Vandersypen, L. M.; Steffen, M.; Breyta, G.; Yannoni, C. S.; Cleve, R.; Chuang, I. L. *Phys. Rev. Lett.* **2000**, *85*, 5452.
(2) Gershenfeld, N. A.; Chuang, I. L. *Science* **1997**, *275*, 350.
(3) Warren, W. S. *Science* **1997**, *277*, 1688.
(4) Marx, R.; Fahmy, A. F.; Myers, J. M.; Bermel, W.; Glaser, S. J. *Phys. Rev. A* **2000**, *62*, 012310.
(5) Gräfenstein, J.; Cremer, D. *J. Chem. Phys.* **2007**, *127*, 174704.
(6) Mawhinney, R. C.; Schreckenbach, G. *Magn. Reson. Chem.* **2004**, *42*, 88.
(7) Biesemans, M.; Martins, J. C.; Jurkschat, K.; Pieper, N.; Seemeyer, S.; Willem, R. *Magn. Reson. Chem.* **2004**, *42*, 776.
(8) Alonso, M. A.; Casares, J. A.; Espinet, P.; Martínez-Ilarduya, J. M.; Pérez-Briso, C. *Eur. J. Inorg. Chem.* **1998**, 1745.
(9) Albéniz, A. C.; Casado, A. L.; Espinet, P. *Organometallics* **1997**, *16*, 5416.
(10) Pogodin, S.; Rae, I. D.; Agranat, I. *Eur. J. Org. Chem.* **2006**, 5059.
(11) Krcsmar, L.; Grunenberg, J.; Dix, I.; Jones, P. G.; Ibrom, K.; Ernst, L. *Eur. J. Org. Chem.* **2005**, 5306.
(12) Gholivand, K.; Ghadimi, S.; Naderimanesh, H.; Forouzanfar, A. *Magn. Reson. Chem.* **2001**, *39*, 684.
(13) Hennig, M.; Munzarová, M. L.; Bermel, W.; Scott, L. G.; Sklenář, V.; Williamson, J. R. *J. Am. Chem. Soc.* **2006**, *128*, 5851.
(14) Gräfenstein, J.; Tuttle, T.; Cremer, D. *Phys. Chem. Chem. Phys.* **2005**, *7*, 452.
(15) Aucar, G. A. *Magn. Reson. Chem. A* **2008**, *32*, 88.
(16) Peruchena, N. M.; Aucar, G. A.; Contreras, R. H. *J. Mol. Struct. (Theochem)* **1990**, *210*, 205.

10.1021/ic801940h CCC: $40.75 
Published on Web 04/01/2009

**Chart 1.** Examples of Compounds Exhibiting Long-Rang Through-Space (**I,III**)[8,9] and Through-Bond $^{19}F-^{19}F$ (**II**) and $^{31}P-^{1}H$ (**IV**) Coupling[a]

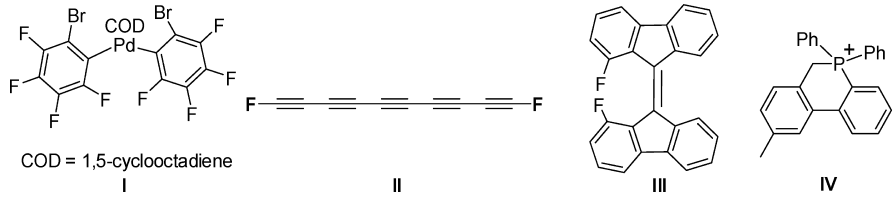


[a] Compounds exhibiting long-range homonuclear through-space or through-bond spin couplings. **I**: $^{6}J_{FF} = 52$ Hz.[8,9] **II**: $^{11}J_{FF} = 7.3$ Hz.[17] **III**: $^{7}J_{FF} = 11.0$ Hz.[10,11] **IV**: $^{7}J_{PH} = 0.4$ Hz.[12]

**Chart 2.** Examples of Platinum Heteronuclear Spin Systems[a]

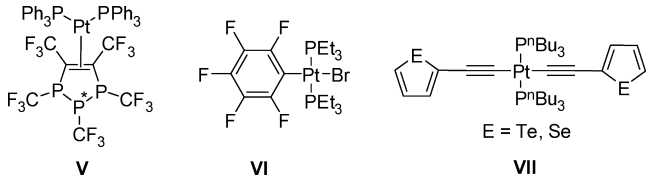


[a] The $^{19}F$ atoms of the unique $P^*CF_3$ moiety of **V** are coupled through-space to $^{195}Pt$. **V**: $J_{PtF} = 11$ Hz.[19] **VI**: $^{5}J_{PtF} = 18$ Hz.[21,22] **VII**: $^{4}J_{PtSe} = 27$ Hz and $^{4}J_{PtTe} = 57$ Hz.[20]

**Chart 3.** Complexes **1**−**4** Showing Unusual Long-Range $^{195}Pt-^{19}F$ and $^{31}P-^{19}F$ Through-Bond Spin Coupling in Solution (Table 1)

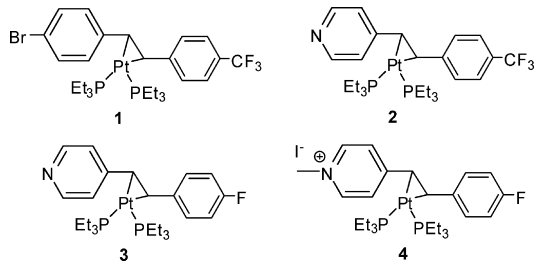


**V**,[19] whereas through-bond $^{195}Pt-^{19}F$ and $^{195}Pt-E$ (E = $^{77}Se$, $^{125}Te$) communication is observed in complexes **VI** and **VII**, respectively.[20−22]

Herein, we report on the formation of four new stilbene- (Chart 3, **1**) and stilbazole-based platinum complexes (**2**−**4**) having long-range $^{195}Pt-^{19}F$ spin coupling through six (**3**, **4**) and seven bonds (**1**, **2**) and long-range $^{31}P-^{19}F$ spin coupling through seven (**3**, **4**) and eight bonds (**1**, **2**). Single-crystal X-ray crystallography analysis and solution NMR studies are consistent with through-bond heteronuclear interactions rather than through-space communication. The experimental and simulated $^{19}F\{^{1}H\}$, $^{31}P\{^{1}H\}$, and $^{195}Pt\{^{1}H\}$ NMR spectra show that these new complexes exhibit either five-spin $AMY_3$ (**1**, **2**) or three-spin AMY (**3**, **4**) systems flanked by six-spin $AMXY_3$ (for **1**, **2**) or four-spin AMXY (for **3**, **4**) systems with A and M = $^{31}P$, X = $^{195}Pt$, and Y = $^{19}F$ resulting from satellites from $^{195}Pt$ (natural abundance 33.8%).[23]

**Table 1.** Long Range $^{195}Pt-^{19}F$ and $^{31}P-^{19}F$ Coupling Constants for Complexes **1**−**4**[a]

| | $^{195}Pt-^{19}F$ coupling[b] in Hz | distance ($^{195}Pt-^{19}F$) in nm | $^{31}P-^{19}F$ coupling[c] in Hz | distance ($^{31}P-^{19}F$) in nm |
|---|---|---|---|---|
| **1** | $^{7}J_{PtF} = 13.2$ | 1.1 | $^{8}J_{PF(trans)} = 3.1$[d] | 1.3 |
| **2** | $^{7}J_{PtF} = 11.8$ | 1.1 | $^{8}J_{PF(trans)} = 2.9$[d] | 1.3 |
| **3** | $^{6}J_{PtF} = 11.6$ | 0.9 | $^{7}J_{PF(trans)} = 3.5$; $^{7}J_{PF(cis)} = 0.4$ | 1.1 |
| **4** | $^{6}J_{PtF} = 40.1$ | 0.9 | $^{7}J_{PF(trans)} = 3.2$[d] | 1.1 |

[a] The through-bond distances were estimated from the X-ray structures of complexes **2** and **3**. [b] Determined by both $^{195}Pt\{^{1}H\}$ and $^{19}F\{^{1}H\}$ NMR spectroscopy. [c] Determined by $^{19}F\{^{1}H\}$ and $^{31}P\{^{1}H\}$ NMR spectroscopy. [d] $^{8}J_{PF(cis)}$ was not observed.

## Experimental Section

**Materials and Methods.** All reactions were carried out in a $N_2$-filled M. Braun glovebox with $H_2O$ and $O_2$ levels <2 ppm. Reagent grade or better solvents were dried, distilled, and degassed before introduction into the glovebox where they were stored over activated 4 Å molecular sieves. Deuterated solvents were purchased from Aldrich and were degassed and stored over 4 Å activated molecular sieves in the glovebox. Reaction flasks were washed with deionized (DI) water followed by acetone, and then oven dried prior to use. Mass spectrometry was carried out using a Micromass Platform LCZ 4000 mass spectrometer. Elemental analyses were performed by H. Kolbe of Mikroanalytisches Laboratorium, Mülheim an der Ruhr, Germany. Ligands **5**−**8** (Scheme 1) and $Pt(PEt_3)_4$ were prepared according to published procedures.[24−27]

**Spectroscopic Analysis.** The $^{1}H$, $^{13}C$, $^{15}N$, $^{19}F$, $^{31}P$, and $^{195}Pt$ NMR spectra were recorded at 500.132, 125.77, 50.69, 470.05, 202.46, and 107.52 MHz, respectively, on a Bruker Avance 500 NMR spectrometer. Certain additional NMR experiments were done on a Bruker Avance 400 MHz spectrometer. All chemical shifts ($\delta$) are reported in ppm and all coupling constants ($J$) in Hz. The $^{1}H$ and $^{13}C$ NMR chemical shifts are reported relative to tetramethylsilane. The resonances of the residual protons of the solvent (7.15 ppm benzene, 7.09 ppm toluene, 3.58 and 1.73 ppm tetrahydrofuran, 2.04 ppm acetone) and of the *d* solvent peaks (128.0 ppm benzene, 20.4 ppm toluene, 67.6 and 25.3 ppm tetrahydrofuran, 29.8 ppm acetone), respectively, were used as the internal standards. $^{31}P\{^{1}H\}$ NMR chemical shifts are relative to 85% $H_3PO_4$ in $D_2O$. $^{195}Pt\{^{1}H\}$ NMR chemical shifts were referenced to $Na_2PtCl_6$ (external standard $K_2PtCl_4$ in $D_2O$ (1.2 M) at $\delta = -1620$ ppm).[28] $^{15}N$ NMR chemical shifts were referenced to liquid $NH_3$. All measurements were carried out at 298 K unless stated otherwise.

(17) Provasi, P. F.; Aucar, G. A.; Sauer, S. P. A. *J. Phys. Chem. A* **2004**, *108*, 5393.
(18) Ernst, L.; Ibrom, K. *Angew. Chem., Int. Ed.* **1995**, *34*, 1881.
(19) Phillips, I. G.; Ball, R. G.; Cavell, R. G. *Inorg. Chem.* **1987**, *26*, 4074.
(20) James, E. C.; Jura, M.; Kociok-Köhn, G.; Raithby, P. R.; Sharp, E. L.; Wilson, P. J. *Inorg. Chem.* **2007**, *46*, 7232.
(21) Pregosin, P. S. *Stud. Inorg. Chem.* **1991**, *13*, 216.
(22) Hopton, F. J.; Rest, A. J.; Rosevear, D. T.; Stone, F. G. A. *J. Chem. Soc.* **1966**, 1326.
(23) *CRC Handbook of Chemistry and Physics*, 83rd ed.; Lide, D. R., Ed.; CRC Press: Boca Raton, FL, 2002−2003.
(24) Gascoyne, J. M.; Mitchell, P. J.; Phillips, L. *J. Chem. Soc., Perkin Trans. 2* **1977**, 1051.
(25) Yoshida, T.; Matsuda, T.; Otsuka, S. *Inorg. Synth.* **1979**, *19*, 110.
(26) Aun, C. E.; Clarkson, T. J.; Happer, D. A. R. *J. Chem. Soc., Perkin Trans. 2* **1990**, *4*, 645.
(27) Schunn, R. A. *Inorg. Chem.* **1976**, *15*, 208.
(28) *Encyclopedia of Spectroscopy and Spectrometry*; Tranter G. E., Holmes J. L., Lindon J. C., Eds.; Academic Press: San Diego, CA, 2000; p 720.

**Scheme 1.** Room Temperature Reaction of Ligands **5**−**8** in THF with $Pt(PEt_3)_4$ Results in Selective $\eta^2$-Coordination of the Central Carbon−Carbon Double Bond to $Pt(PEt_3)_2$ (**1**−**4**)[a]

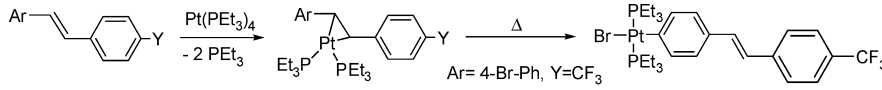


**5** Ar = 4-Br-Ph,Y=$CF_3$
**6**, Ar = Pyr,Y=$CF_3$
**7**, Ar = Pyr, Y=F
**8**, Ar = Pyr•MeI, Y=F

**1**, Ar = 4-Br-Ph,Y=$CF_3$
**2**, Ar = Pyr,Y=$CF_3$
**3**, Ar = Pyr, Y=F
**4**, Ar = Pyr•MeI, Y=F

**9**

[a] Compound **1** undergoes selective activation of the aryl−bromide bond to afford complex **9**.

Assignments in the $^1H$ and $^{13}C$ NMR were made using $^1H\{^{31}P\}$ and $^{13}C$-DEPT135 NMR. The 2D $^{15}N-^1H$ gsHMBC heteronuclear shift correlation spectra were acquired and processed using standard Bruker software.[29]

**Formation of Complex 1.** A solution of $Pt(PEt_3)_4$ (44.1 mg, 0.066 mmol) in 1 mL of THF was mixed with a solution of *E*-1-[(2-(4-bromophenyl)ethenyl]-4-(trifluoromethyl)-benzene (**5**)[24] (21.6 mg, 0.066 mmol) in 2 mL of THF at room temperature. Quantitative formation of complex **1** was observed by $^{31}P\{^1H\}$ NMR spectroscopy after stirring for 20 min. Complex **1** was isolated as a white solid by removing all volatiles under vacuum and by washing the residue with 5 mL of dry pentane. Complex **1** was stored at −30 °C as a solid. $^1H$ NMR (THF-$d_8$): $\delta$ 7.28 (d, 2H, ArH, $^3J_{HH}$ = 8.0 Hz), 7.16 (d, 2H, ArH, $^3J_{HH}$ = 7.8 Hz), 7.11 (d, 2H, ArH, $^3J_{HH}$ = 7.8 Hz), 6.95 (d, 2H, ArH, $^3J_{HH}$ = 7.6 Hz), 3.67−3.57 (m, 2H, CH═CH, $^1J_{PtH}$ = 52.7 Hz), 1.65 (m, 12H, P$CH_2$$CH_3$), 0.89 (m, 18H, $PCH_2CH_3$). $^{13}C\{^1H\}$ NMR ($C_6D_6$): $\delta$ 153.85 (d, $C_q$, $^2J_{PtC}$ = 42.3 Hz, $^3J_{PC}$ = 6.5 Hz), 147.54 (d, $C_q$, $^2J_{PtC}$ = 40.0 Hz, $^3J_{PC}$ = 6.2 Hz, $^3J_{PC}$ = 2.1 Hz), 132.10, 130.70 (d, $^5J_{PC}$ = 1.9 Hz), 128.53, 127.19 (d, $^3J_{PtC}$ = 20.4 Hz, $^4J_{PC}$ = 3.2 Hz), 126.9 (s, $C_q$), 125.82 (m, $C_q$, $CF_3$, $^1J_{CF}$ = 3.9 Hz), 125.03 (d, $^3J_{PtC}$ = 20.1 Hz, $^4J_{PC}$ = 2.9 Hz), 124.67 (br), 115.9 (d, $C_q$, C−Br), 50.97 (d, $\eta^2$-CH═CH, $^1J_{PtC}$ = 208.6, $^2J_{PC}$ = 34.3 Hz), 50.29 (d, $\eta^2$-CH═CH, $^1J_{PtC}$ = 208.5, $^2J_{PC}$ = 32.7 Hz), 20.15 (m, P$CH_2$$CH_3$, $^2J_{PtC}$ = 65.7, $^1J_{PC}$ = 35.0, $^3J_{PC}$ = 3.4 Hz), 8.35 (d, $PCH_2CH_3$, $^3J_{PC}$ = 36.1, $^2J_{PC}$ = 12.4 Hz). $^{31}P\{^1H\}$ NMR ($C_6D_6$): AM part of $AMY_3$ system flanked by AM part of $AMXY_3$ system, $\delta_A$ 13.49 (1P, $^2J_{PP}$ = 44.4, $^1J_{PtP}$ = 3583.6, $^8J_{PF}$ = 3.1 Hz), $\delta_M$ 12.97 (1P, $^2J_{PP}$ = 44.4, $^1J_{PtP}$ = 3518.8 Hz). $^{195}Pt\{^1H\}$ NMR ($C_6D_6$, 107.04 MHz): X part of $AMXY_3$ system, $\delta$ −5086.1 (1Pt, $^1J_{PPt}$ = 3518.8, $^1J_{PPt}$ = 3583.5 Hz). $^{19}F\{^1H\}$ NMR ($C_6D_6$): d, Y part $AMY_3$ system flanked by Y part of $AMXY_3$ system, $\delta_Y$ −61.03 (3F, $^7J_{PtF}$ = 13.2, $^8J_{PF}$ = 3.1 Hz). Elemental analysis (%) calcd for $C_{27}H_{40}BrF_3P_2Pt$: C 42.75, H 5.32. Found: C 42.94, H 5.20.

**Formation of Complex 9.** A solution of complex **1** (21.5 mg, 0.028 mmol) in 1 mL of THF was loaded into a 5 mm screw-cap NMR tube, which was sealed using Teflon tape and parafilm. The reaction progress was monitored by $^{31}P\{^1H\}$ NMR spectroscopy showing the formation of complex **9** and concurrent disappearing of the starting material (**1**). After ∼30 min at 58 °C formation of complex **9** became visible, whereas complex **1** disappeared. No intermediates were observed. The reaction was nearly completed in 8 h (∼96% conversion). Complex **9** was the only observable product and was isolated (87%) as a light-yellow solid by removing all volatiles under vacuum followed by washing of the residue with 2 mL of cold (−30 °C) pentane. $^1H$ NMR ($C_6D_6$): $\delta$ 7.67 (d, 2H, ArH, $^3J_{HH}$ = 8.3 Hz), 7.60 (d, 2H, ArH, $^3J_{HH}$ = 8.4 Hz), 7.39 (d, 2H, ArH, $^3J_{HH}$ = 7.9 Hz), 7.27 (d, CH═CH, 1H, $^3J_{HH}$ = 16.9 Hz), 7.16 (d, 2H, ArH, $^3J_{HH}$ = 8.6 Hz), 7.11 (d, CH═CH, 1H, $^3J_{HH}$ = 16.1 Hz), 1.74 (m, 12H, P$CH_2$$CH_3$), 1.08 (m, 18H, $PCH_2CH_3$). $^{13}C\{^1H\}$ NMR (acetone-$d_6$): $\delta$ 145.36 (t, $C_q$, $^2J_{PC}$ = 18.45, $^1J_{PtC}$ = 945 Hz), 142.10 (s, $C_q$), 139.31 (s, $^2J_{PtC}$ = 38.8 Hz), 134.45, 132.28 (s, $C_q$), 131.24 (s, $C_q$), 126.82 (m, $C_q$, $^1J_{CF}$ = 3.5 Hz, $CF_3$), 128.27, 128.02, 127.36, 125.36, 15.73 (vt, $^{1+3}J_{PC}$ = 34.21, $^2J_{PtC}$ = 69.5 Hz), 8.01 (s, $^3J_{PtC}$ = 25.2 Hz). $^{31}P\{^1H\}$ NMR ($C_6D_6$): $\delta$ 10.20 (s, 2P, $^1J_{PtP}$ = 2764.0 Hz). $^{195}Pt\{^1H\}$ NMR ($C_6D_6$, 107.04 MHz): $\delta$ −4476.4 (s, 1Pt, $^1J_{PPt}$ = 2764.4 Hz). $^{19}F\{^1H\}$ NMR ($C_6D_6$): $\delta$ −62.06 (s). Elemental analysis (%) calcd for $C_{27}H_{40}BrF_3P_2Pt$: C 42.75, H 5.32. Found: C 42.49, H 5.26.

**Formation of Complex 2.** $Pt(PEt_3)_4$ (56 mg, 0.083 mmol) was dissolved in 3 mL of dry THF and slowly added to a stirred solution of *E*-4-[2-(4-trifluoromethyl-phenyl)-ethenyl]-pyridine (**6**)[26] (21 mg, 0.083 mmol) in 2 mL of THF. After stirring at room temperature for 20 min, all volatiles were removed under vacuum, and the residue was washed with 10 mL of pentane. The yellow residue was dissolved in ∼1.5 mL of THF, which was followed by dropwise addition of ∼9 mL of dry pentane. Slow evaporation of the solvent at room temperature resulted after 6 days in the formation of colorless needle-like crystals of analytically pure complex **2** (75% yield). $^1H$ NMR ($C_6D_6$): $\delta$ 8.52 (d, 2H, ArH, $^3J_{HH}$ = 5.4 Hz), 7.36 (d, 2H, ArH, $^3J_{HH}$ = 8.1 Hz), 7.02 (d, 2H, ArH, $^3J_{HH}$ = 7.8 Hz), 6.87 (d, 2H, ArH, $^3J_{HH}$ = 4.5 Hz), 3.78−3.52 (m, 2H, CH═CH, $^2J_{PtH}$ = 52.3 Hz), 1.23 (m, 12H, P$CH_2$$CH_3$), 0.66 (m, 18H, $PCH_2CH_3$). $^{13}C\{^1H\}$ NMR ($C_6D_6$): $\delta$ 156.86 (d, $C_q$, $^2J_{PtC}$ = 40.6, $^3J_{PC}$ = 5.3 Hz), 153.2 (d, $C_q$, $^2J_{PtC}$ = 38.2, $^3J_{PC}$ = 5.6 Hz), 149.13 (br d, $^5J_{PC}$ = 1.9 Hz), 128.59, 125.03 (d, $^3J_{PtC}$ = 19.4, $^4J_{PC}$ = 2.9 Hz), 125.57 (m, $C_q$, $CF_3$, $^1J_{FC}$ = 3.9 Hz), 124.47 (m), 124.21 (br, $C_q$), 120.02 (d, $^3J_{PtC}$ = 17.9, $^4J_{PC}$ = 2.3 Hz), 49.30 (d, $\eta^2$-CH═CH, $^1J_{PtC}$ = 210, *trans*-$^2J_{PC}$ = 32.9 Hz), 48.74 (d, $\eta^2$-CH═CH, $^1J_{PtC}$ = 205, *trans*-$^2J_{PC}$ = 31.7 Hz), 19.67 (m, P$CH_2$$CH_3$, $^2J_{PtC}$ = 57.3, $^1J_{PC}$ = 22.4, $^4J_{PC}$ = 3.4 Hz), 8.10 (d, $PCH_2CH_3$, $^3J_{PtC}$ = 23.3, $^2J_{PC}$ = 18.3 Hz). $^{31}P\{^1H\}$ NMR ($C_6D_6$): AM part of $AMY_3$ system flanked by AM part of $AMXY_3$ system, $\delta_A$ 14.46 (1P, $^2J_{PP}$ = 39.8, $^1J_{PtP}$ = 3591.1 Hz), $\delta_M$ 14.09 (1P, $^2J_{PP}$ = 39.8, $^7J_{PF}$ = 2.9, $^1J_{PtP}$ = 3539.0 Hz). $^{195}Pt\{^1H\}$ NMR ($C_6D_6$, 107.04 MHz): X part of $AMXY_3$ system, $\delta$ −5084.3 (1Pt, $^7J_{PtF}$ = 11.8, $^1J_{PPt}$ = 3591.1, $^1J_{PPt}$ = 3538.4 Hz). $^{19}F\{^1H\}$ NMR ($C_6D_6$): d, Y part $AMY_3$ system flanked by Y part of $AMXY_3$ system, $\delta_Y$ −60.97 (3F, $^7J_{PtF}$ = 11.8, $^8J_{PF}$ = 2.9 Hz). $^{15}N$ NMR (acetone-$d_6$): $\delta$ 298.0 (s). UV−vis ($CH_3CN$) $\lambda(\epsilon)$ 318 nm ($1.7 \times 10^4$ $M^{-1}cm^{-1}$). Calcd *m*/*e*: 680.6, found 681.8. Anal. Calcd for $C_{26}H_{40}F_3NP_2Pt$: C 45.88, H 5.92. Found: C 45.79, H 5.95.

**Formation of Complex 3.** $Pt(PEt_3)_4$ (41.3 mg, 0.062 mmol) was dissolved in 3 mL of dry THF and slowly added to a stirred solution of *E*-4-[2-(4-fluoro-phenyl)-ethenyl]-pyridine (**7**)[26] (12.3 mg, 0.062 mmol) in 2 mL of THF. After stirring at room temperature for 20 min, the volatiles were removed under vacuum, and the residue was washed with 4 mL of pentane. The yellow residue was dissolved in ∼1.5 mL of THF, which was followed by dropwise addition of ∼6 mL of dry pentane. Slow evaporation of the solvent at room temperature resulted after 5 days in the formation of colorless needle-like crystals of analytically pure complex **3** (85% yield). $^1H$ NMR ($C_6D_6$): $\delta$ 8.52 (d, 2H, ArH, $^3J_{HH}$ = 6.0 Hz), 7.00

(29) Von Philipsborn, W.; Müller, R. *Angew. Chem., Int. Ed.* **1986**, *25*, 383.

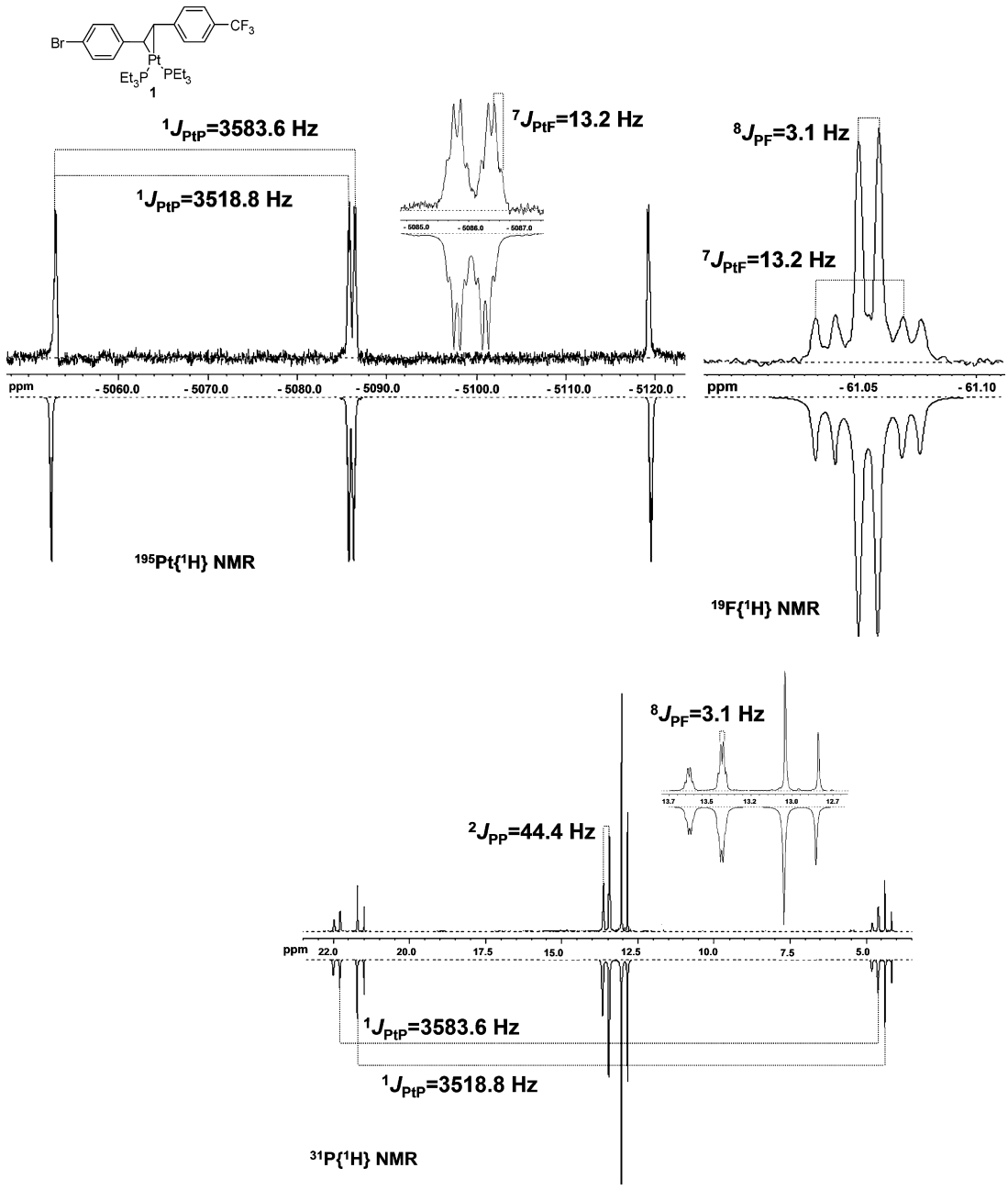


**Figure 1.** Experimental (upper) and simulated (lower) $^{31}P\{^1H\}$, $^{19}F\{^1H\}$, and $^{195}Pt\{^1H\}$ NMR spectra of complex **1** in acetone-$d_6$ showing the $AMY_3$ spin system flanked by $AMXY_3$ spin system (A, M = $^{31}P$, X = $^{195}Pt$ and Y = $^{19}F$). The simulated spectra were obtained with gNMR (version 5.0).[59]

(m, 2H, ArH, $^3J_{HH}$ = 5.4 Hz), 6.89 (m, 2H, ArH), 6.88 (m, br, 2H, ArH), 3.79−3.52 (m, 2H, CH═CH, $^2J_{PtH}$ = 52.8 Hz), 1.27 (m, 12H, $PCH_2CH_3$), 0.70 (m, 18H, $PCH_2CH_3$). $^{13}C\{^1H\}$ NMR ($C_6D_6$): $\delta$ 160.12 (d, $C_q$), 157.03 (dd, $C_q$, $^2J_{PtC}$ = 43.1, $^3J_{PC}$ = 6.0, $^3J_{PC}$ = 2.6 Hz), 144.65 (dd, $C_q$, $^2J_{PtC}$ = 37.7, $^3J_{PC}$ = 5.3, $^3J_{PC}$ = 2.7 Hz), 149.08 (d, $J_{PC}$ = 1.7 Hz), 126.45, (d, $^3J_{PtC}$ = 27.5, $^4J_{PC}$ = 3.4 Hz), 119.88 (d, $^3J_{PtC}$ = 18.6, $^4J_{PC}$ = 2.7 Hz), 114.02, 114.19, 50.13 (d, $\eta^2$-CH═CH, $^1J_{PtC}$ = 206.1, *trans*-$^2J_{PC}$ = 36.6 Hz), 50.43 (d, $\eta^2$-CH═CH, $^1J_{PtC}$ = 205.1, *trans*-$^2J_{PC}$ = 36.6 Hz), 19.7 (dd, $PCH_2CH_3$, $^2J_{PtC}$ = 50.5, $^1J_{PC}$ = 16.5, $^4J_{PC}$ = 2.7 Hz), 8.10 (d, $PCH_2CH_3$, $^2J_{PC}$ = 2.5, $^3J_{PtC}$ = 21.2 Hz). $^{31}P\{^1H\}$ NMR ($C_6D_6$): AM part of AMY system flanked by AM part of AMXY system, $\delta_A$ 15.28 (1P, $^2J_{PP}$ = 44.3, $^1J_{PtP}$ = 3639.9 Hz), $\delta_M$ 14.40 (1P, $^2J_{PP}$ = 44.3, $^7J_{PF}$ = 3.5, $^1J_{PtP}$ = 3465.7 Hz). $^{195}Pt\{^1H\}$ NMR ($C_6D_6$, 107.04 MHz): X part of AMXY system, $\delta_X$ −5087.3 (1Pt, $^6J_{PtF}$ = 11.6, $^1J_{PPt}$ = 3639.7, $^1J_{PPt}$ = 3465.4 Hz). $^{19}F\{^1H\}$ NMR (acetone-$d_6$): d, Y part AMY system flanked by Y part of AMXY system, $\delta_Y$ −123.30 (1F, $^6J_{PtF}$ = 11.6, *trans*-$^7J_{PF}$ = 3.5, *cis*-$^7J_{PF}$ = 0.4 Hz). $^{15}N$ NMR (acetone-$d_6$): $\delta$ 296.3 (s). UV−vis ($CH_3CN$) $\lambda(\epsilon)$ 307 nm ($2.6 \times 10^4$ $M^{-1}cm^{-1}$). Calcd *m/e*: 630.2, found 631.8. Elemental analysis (%) calcd for $C_{25}H_{40}FP_2Pt$: C 47.65, H 6.39, N 2.22. Found: C 48.23, H 6.54, N 2.22.

**Formation of Complex 4.** $Pt(PEt_3)_4$ (33.2 mg, 0.050 mmol) was dissolved in 3 mL of dry THF and slowly added to a stirred solution of 4-[2-(4-fluoro-phenyl)-ethenyl]-1-methyl-pyridinium iodide (**8**)[26] (17 mg, 0.050 mmol) in 3 mL of THF. After stirring at room temperature for 1 h, the volatiles were removed under vacuum, and the residue was washed with dry pentane (2 × 3 mL). Complex **4** was isolated as yellow sticky oil in 95% yield by removing all volatiles under vacuum. $^1H$ NMR (acetone-$d_6$), 223 K: $\delta$ 7.58 (br, 2H), 7.20 (t, 2H, ArH, $^3J_{HH}$ = 5.9 Hz), 7.02 (t, 2H, ArH, $^3J_{HH}$ = 8.8 Hz), 6.91 (br, 2H, ArH), 4.09 (br, 3H, *N*-$CH_3$), 4.21−3.60 (m, 2H, CH═CH, $^2J_{PtH}$ = 50.8 Hz), 1.71 (m, 12H, $PCH_2CH_3$), 0.88 (m, 18H, $PCH_2CH_3$). $^{13}C\{^1H\}$ NMR (acetone-$d_6$), 223 K: $\delta$ 163.44

(dd, $C_q$, br, $^2J_{PtC}$ = 44.5, $^3J_{PC}$ = 1.6 Hz), 161.7 (d, $C_q$), 159.21, 142.52 (dd, $C_q$, $^2J_{PtC}$ = 29.7, $^3J_{PC}$ = 6.1, $^3J_{PC}$ = 2.6 Hz), 127.07, (m, br, $^4J_{PC}$ = 6.1, $^4J_{PC}$ = 2.7 Hz), 114.36, 114.19, 54.15 (d, $\eta^2$-CH═CH, $^1J_{PtC}$ = 110.5, *trans*-$^2J_{PC}$ = 20.9 Hz), 48.65 (d, $\eta^2$-CH═CH, $^1J_{PtC}$ = 220.8, *trans*-$^2J_{PC}$ = 35.6 Hz), 44.61 (*N*-$CH_3$), 18.42−17.48 (m, P$CH_2CH_3$, $^1J_{PC}$ = 61.9, $^4J_{PC}$ = 28.1 Hz), 8.10 (d, $PCH_2CH_3$, $^2J_{PC}$ = 18.9, $^3J_{PtC}$ = 28.4 Hz). $^{31}P\{^1H\}$ NMR (acetone-$d_6$): AM part of AMY system flanked by AM part of AMXY system, $\delta_A$ 15.45 (1P, $^2J_{PP}$ = 22.9, $^1J_{PtP}$ = 4022.9 Hz), $\delta_M$ 11.74 (1P, $^2J_{PP}$ = 22.7, $^1J_{PtP}$ = 3329.8, $^7J_{PF}$ = 3.2 Hz). Two isomers were observed by $^{195}Pt\{^1H\}$ NMR spectroscopy. $^{195}Pt\{^1H\}$ NMR ($C_6D_6$, 107.04 MHz): br ($\omega_{1/2}$ = 50 Hz), X part of AMXY system, $\delta$ −5005.1 (1Pt, $^1J_{PPt}$ = 3329.5, $^1J_{PPt}$ = 4023.1 Hz; major signal, 70%) and br ($\omega_{1/2}$ = 50 Hz), X part of AMXY system, $\delta_X$ −5007.1 (1Pt, $^1J_{PPt}$ = 3329.5, $^1J_{PPt}$ = 4023.1 Hz; minor signal, 30%). $^{19}F\{^1H\}$ NMR (acetone-$d_6$), 223 K: m, Y part AMY system flanked by Y part of AMXY system, $\delta_Y$ −121.06 (1F, $^6J_{PtF}$ = 40.01, *trans*-$^7J_{PF}$ = 3.2 Hz). $^{15}N$ NMR (acetone-$d_6$): $\delta$ 166.2. UV−vis ($CH_3CN$) $\lambda(\epsilon)$ 399 nm (2.2 × $10^4$ $M^{-1}cm^{-1}$). Calcd *m*/*e*: 772.5, found (M − $I^-$) 646.9. Elemental analysis (%) calcd for $C_{26}H_{43}FIP_2Pt$: C 40.22, H 5.61. Found: C 40.15, H 5.96.

**X-ray Analysis of Complex 2. Crystal Data.** $C_{26}H_{40}NP_2F_3Pt$, 0.4 × 0.1 × 0.1 $mm^3$, monoclinic, space group *P*2(1)/*c*, *a* = 8.921(2) Å, *b* = 11.495(2) Å, *c* = 27.546(6) Å, $\beta$ = 95.54(3)°, *T* = 120(2)K, *V* = 2811.6 (10) $Å^3$, *Z* = 4, Fw = 680.62, Dc = 1.608 $Mg\cdot m^{-3}$, $\mu$ = 5.138 $mm^{-1}$.

**Data Collection and Processing.** Nonius KappaCCD diffractometer, Mo K$\alpha$ ($\lambda$ = 0.71073 Å), 17459 reflections collected, 6324 independent reflections ($R_{int}$ = 0.0630). The data were processed with Denzo-Scalepack.

**Solution and Refinement.** Structure solved by SHELXS-90,[30] full matrix least-squares refinement based on $F^2$ with SHELXL-97,[30] 305 parameters with 0 restraints, final *R* = 0.0414 (w*R* = 0.0822) for 6324 reflections with $I > 2\sigma(I)$ and *R* = 0.0636 (w*R* = 0.0881) for all data. Goodness of fit on $F^2$ = 1.042, largest electron density peak = 1.858 $e\cdot Å^{-3}$.

**X-ray Analysis of Complex 3. Crystal Data.** $C_{25}H_{40}NP_2FPt$, 0.3 × 0.04 × 0.04 $mm^3$, triclinic, space group $P\bar{1}$, *a* = 8.6720(2) Å, *b* = 11.2167(5) Å, *c* = 14.6807(6) Å, α = 105.3960(16)°, $\beta$ = 95.855(2)°, $\gamma$ = 104.263(2)°, *Z* = 2, *T* = 120(2) K, *V* = 1312.7 (1) $Å^3$, Fw = 630.60, Dc = 1.595 $Mg\cdot m^{-3}$, $\mu$ = 5.485 $mm^{-1}$.

**Data Collection and Processing.** Nonius KappaCCD diffractometer, Mo K$\alpha$ ($\lambda$ = 0.71073 Å), 25780 reflections collected, 5976 independent reflections ($R_{int}$ = 0.084). The data were processed with Denzo-Scalepack.

**Solution and Refinement.** This structure has been solved by SIR-97.[31] Full matrix least-squares refinement based on $F^2$ with SHELXL-97,[30] 280 parameters with 0 restraints, final *R* = 0.0361 (w*R* = 0.0729) for 5354 reflections with $I > 2\sigma(I)$ and *R* = 0.0511 (w*R* = 0.0765) for all data. Goodness of fit on $F^2$ = 1.015, largest electron density peak = 1.814 $e\cdot Å^{-3}$.

**Computational Details.** All calculations were carried out using Gaussian 03 Revision E.01.[32] The PBE0 (also known as PBE1PBE or PBEh)[33] hybrid Generalized Gradient Approximation (GGA) DFT exchange-correlation functional was used. PBE0 is the Adamo−Barone hybrid variant of the Perdew−Burke−Ernzerhof (PBE) GGA functional[34,35] and contains 25% Hartree−Fock exchange.[33] This functional has been shown to yield more reliable properties for transition metals than other conventional exchange-correlation functionals.[36] The SDD basis set RECP (relativistic effective core potential) combination was used. This combines the Huzinaga−Dunning double-$\zeta$ basis set[37] on lighter elements with the Stuttgart−Dresden basis set RECP combination[38] on transition metals. Diffuse functions were added to the fluorine atom as recommended by Martin and co-workers.[39] Bulk solvent effects were approximated by single-point energy calculations using a polarizable continuum model (PCM),[40−43] specifically the integral equation formalism model (IEF-PCM)[40,41,44,45] with benzene as the solvent as in the experiments.

## Results and Discussion

The reaction of an equimolar amount of $Pt(PEt_3)_4$ with ligands **5**−**8** in dry THF at room temperature for ∼20 min results in the quantitative formation of complexes **1**−**4**, respectively, with concurrent generation of 2 equiv of $PEt_3$ as determined by $^{31}P\{^1H\}$ NMR spectroscopy (Scheme 1). Complex **1** is unstable in solution at room temperature and converts to the product of aryl−Br oxidative addition (**9**) (∼60% conversion in 3 days at room temperature). Thermolysis of complex **1** in THF at elevated temperatures results in quantitative formation of complex **9** within several hours. The $\eta^2$-coordination of the metal center to the carbon−carbon double bond of ligand **5** is kinetically favored over activation of the aryl−halide bond. This transformation (**1**→**9**) may involve an intramolecular ring-walking process,[46−50] as we have observed in structurally related Pt, Pd, and Ni com-

(30) Sheldrick, G. M. *Acta Crystallogr.* **2008**, *A64*, 112.

(31) Altomare, A.; Burla, M. C.; Camalli, M.; Cascarano, G.; C., G.; Guagliardi, A.; Moliterni, A. G. G.; Polidori, G.; Spagna, R. *J. Appl. Crystallogr.* **1994**, *27*, 435.

(32) Frisch, M. J.; Trucks, G. W.; Schlegel, H. B.; Scuseria, G. E.; Robb, M. A.; Cheeseman, J. R.; Montgomery, J.; Vreven, T.; Kudin, K. N.; Burant, J. C.; Millam, J. M.; Iyengar, S. S.; Tomasi, J.; Barone, V.; Mennucci, B.; Cossi, M.; Scalmani, G.; Rega, N.; Petersson, G. A.; Nakatsuji, H.; Hada, M.; Ehara, M.; Toyota, K.; Fukuda, R.; Hasegawa, J.; Ishida, M.; Nakajima, T.; Honda, Y.; Kitao, O.; Nakai, H.; Klene, M.; Li, X.; E., K. J.; Hratchian, H. P.; Cross, J. B.; Bakken, V.; Adamo, C.; Jaramillo, J.; Gomperts, R.; Stratmann, R. E.; Yazyev, O.; Austin, A. J.; Cammi, R.; Pomelli, C.; Ochterski, J. W.; Ayala, P. Y.; Morokuma, K.; Voth, G. A.; Salvador, P.; Dannenberg, J. J.; Zakrzewski, V. G.; Dapprich, S.; Daniels, A. D.; Strain, M. C.; Farkas, O.; Malick, D. K.; Rabuck, A. D.; Raghavachari, K.; Foresman, J. B.; Ortiz, J. V.; Cui, Q.; Baboul, A. G.; Clifford, S.; Cioslowski, J.; Stefanov, B. B.; Liu, G.; Liashenko, A.; Piskorz, P.; Komaromi, I.; Martin, R. L.; Fox, D. J.; Keith, T.; Al-Laham, M. A.; Peng, C. Y.; Nanayakkara, A.; Challacombe, M.; Gill, P. M. W.; Johnson, B.; Chen, W.; Wong, M. W.; Gonzalez, C.; Pople, J. A. *Gaussian 03*; Revision E.01; Gaussian, Inc.: Wallingford, CT, 2004.

(33) Adamo, C.; Barone, V. *J. Chem. Phys.* **1999**, *110*, 6158.

(34) Perdew, J. P.; Burke, K.; Ernzerhof, M. *Phys. Rev. Lett.* **1996**, *77*, 3865.

(35) Perdew, J. P.; Burke, K.; Ernzerhof, M. *Phys. Rev. Lett.* **1997**, *78*, 1396.

(36) Quintal, M. M.; Karton, A.; Iron, M. A.; Boese, A. D.; Martin, J. M. L. *J. Phys. Chem. A* **2006**, *110*, 709.

(37) Dunning, T. H., Jr.; Hay, P. J. *Modern Theoretical Chemistry*, Vol. 3: Methods of Electronic Structure Theory, Schaefer, H. F., III. Ed.; Plenum Press: New York, 1977; pp 1–23.

(38) Dolg, M. *Modern Methods and Algorithms of Quantum Chemistry*; Grotendorst, J., Ed.; John von Neumann Institute for Computing: Jülich, 2000; Vol. 3, pp 507–540.

(39) Parthiban, S.; de Oliveira, G.; Martin, J. M. L. *J. Phys. Chem. A* **2001**, *105*, 895.

(40) Cances, E.; Mennucci, B.; Tomasi, J. *J. Chem. Phys.* **1997**, *107*, 3032.

(41) Mennucci, B.; Tomasi, J. *J. Chem. Phys.* **1997**, *106*, 5151.

(42) Cossi, M.; Barone, V.; Mennucci, B.; Tomasi, J. *Chem. Phys. Lett.* **1998**, *286*, 253.

(43) Cossi, M.; Scalmani, G.; Rega, N.; Barone, V.; Phys., J. C. *J. Chem. Phys.* **2002**, *117*, 43.

(44) Mennucci, B.; Cances, E.; Tomasi, J. *J. Phys. Chem.* **1997**, *101*, 10506.

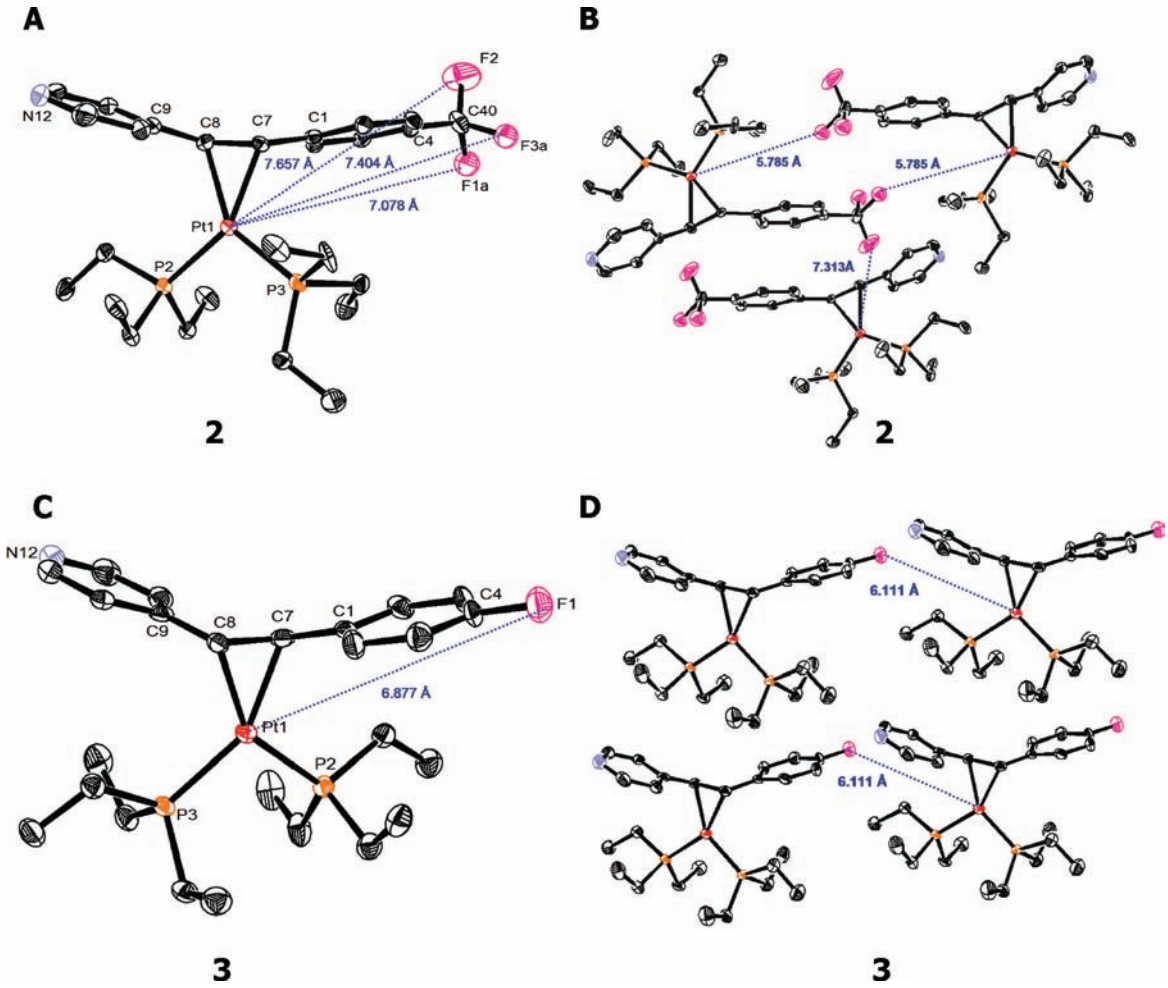


**Figure 2.** (A) ORTEP diagram of complex **2** with thermal ellipsoids set at 50% probability showing the $\eta^2$-coordination of the $Pt(PEt_3)_2$ group to the carbon−carbon double bond, C(7)−C(8). Hydrogen atoms have been omitted for clarity. The dotted blue lines indicate the intramolecular Pt−F distances. There is partial disorder in the fluorine atoms positions, and only one conformation is shown. Selected bond lengths (Å) and angles (°): Pt(1)−C(7) 2.116(5), Pt(1)−C(8) 2.140(5), Pt(1)−P(2) 2.271(1), Pt(1)−P(3) 2.267(1), C(8)−C(7) 1.472(6), C(8)−C(9) 1.466(7), C(1)−C(7) 1.463(7), C(40)−F(1A) 1.34(1), C(40)−F(3A) 1.36(1), C(40)−F(2) 1.318(7), C(7)−Pt(1)−P(2) 151.43(12), C(7)−Pt(1)−C(8) 40.47(17), C(7)−Pt(1)−P(3) 102.81(12), C(8)−Pt(1)−P(2) 110.97(13), P(2)−Pt(1)−P(3) 105.76(5). (B) Perspective view of the intermolecular Pt−F distances (dotted blue lines) in complex **2**. (C) ORTEP diagram of complex **3** with thermal ellipsoids set at 50% probability showing the $\eta^2$-coordination of the $Pt(PEt_3)_2$ group to the carbon−carbon double bond, C(7)−C(8). Selected bond lengths (Å) and angles (°): Pt(1)−C(7) 2.114(4), Pt(1)−C(8) 2.118(4), Pt(1)−P(2) 2.2750(13), Pt(1)−P(3) 2.2849(12), C(8)−C(7) 1.447(7), C(8)−C(9) 1.472(7), C(1)−C(7) 1.499(7), C(4)−F(1) 1.363(6), C(7)−Pt(1)−P(2) 106.76(14), C(7)−Pt(1)−C(8) 40.00(19), C(7)−Pt(1)−P(3) 150.39(14), C(8)−Pt(1)−P(2) 146.70(13), P(2)−Pt(1)−P(3) 102.78(5). (D) Perspective view of the intermolecular Pt−F distances (dotted blue lines) in complex **3**.

plexes.[47,51,52] The new complexes **1**−**4** and **9** were isolated (>85% yield) and characterized by $^1H$, $^{13}C\{^1H\}$, $^{19}F\{^1H\}$, $^{31}P\{^1H\}$, and $^{195}Pt\{^1H\}$ NMR spectroscopy and elemental analysis. $^1H\{^{31}P\}$ and $^{13}C$ DEPT135 NMR spectroscopy were used for signal assignment. Complexes **2**−**4** were also characterized by mass spectrometry and UV−vis spectroscopy. In addition, complexes **2** and **3** were characterized by single-crystal X-ray analysis (Figure 2).

The $\eta^2$-coordination of the metal center to the carbon−carbon double bond of ligands **5**−**8** is apparent from the $^1H$ and $^{13}C\{^1H\}$ NMR spectra of the corresponding complexes (**1**−**4**). Complexes **1**−**3** exhibit typical signals at $\delta$ ∼3.6 and $\delta$ 50−52 ppm in the respective NMR spectra (see Supporting Information, Figures S1–S4).[47] The NMR spectra of complex **4** show similar features, but at $\delta$ 3.6−4.2 ppm and at $\delta$ 48.66 and 54.15 ppm, respectively. The CH units of the $\eta^2$-C=C moieties are inequivalent and are coupled with $^{195}Pt$ and with the $^{31}P$ nuclei of both the *cis*- and *trans*-$PEt_3$ ligands.[53] For complexes **1**−**3**, $^1J_{PtC}$ = 202−208 Hz for both $\eta^2$-C=C atoms. The $^1J_{PtC}$ for complex **4** is drastically different for each carbon atom (221 and 111 Hz), indicating enhanced asymmetric binding resulting from the pyridinium moiety.[54,55] This is supported by DFT calculations (vide infra). This asymmetric binding is also expressed in the $^{31}P\{^1H\}$ NMR spectra of complex **4**. The $^{31}P\{^1H\}$ NMR spectra of complexes **1**−**4** show a resonance at $\delta$ ∼14 ppm with *cis*-$^2J_{PP}$= 40−44 Hz (**1**−**3**) and *cis*-$^2J_{PP}$= 23 Hz (**4**) flanked by platinum satellites ($^1J_{PtP}$ = 3330−4023 Hz). The inequivalent

(45) Tomasi, J.; Mennucci, B.; Cances, E. *J. Mol. Struct. (Theochem)* **1999**, 211.
(46) Fryzuk, M. D.; Jafarpour, L.; Kerton, F. M.; Love, J. B.; Rettig, S. J. *Angew. Chem., Int. Ed.* **2000**, *39*, 767.
(47) Strawser, D.; Karton, A.; Zenkina, O. V.; Iron, M. A.; Shimon, L. J. W.; Martin, J. M. L.; van der Boom, M. E. *J. Am. Chem. Soc.* **2005**, *127*, 9322.
(48) Stanger, A.; Vollhardt, K. P. C. *Organometallics* **1992**, *11*, 317.
(49) Miyakoshi, R.; Yokoyama, A.; Yokozawa, T. *J. Am. Chem. Soc.* **2005**, *127*, 17542.
(50) Keane, J. M.; Harman, W. D. *Organometallics* **2005**, *24*, 1786.

P atoms of complex **4** exhibit a ~700 Hz difference in coupling with the Pt center, whereas the two P atoms of complexes **1**−**3** have similar Pt couplings. The $^{31}P\{^1H\}$ NMR resonances of complex **4** are sharp within the temperature range 223−298 K. However, the $^1H$ and $^{19}F\{^1H\}$ NMR spectra were recorded at 223 K because broadened resonances are observed at room temperature. The nature of this line broadening is not clear.

The olefinic carbons in complex **2** are unusually complex in the $^{13}C\{^1H\}$ spectra (see Supporting Information, Figures S1−S4). This results from the non-first-order nature of the spectrum and has been observed in related compounds.[54,55] This is discussed in detail in the accompanying Supporting Information.

The $^{31}P\{^1H\}$ NMR spectrum of complex **9** exhibits one sharp singlet at $\delta$ 10.2 ppm flanked by $^{195}Pt$ satellites as a result of symmetrical equivalence. The observed $^{195}Pt-^{31}P$ coupling, $^1J_{PtP} = 2764$ Hz, is typical of two mutually *trans* phosphorus atoms bound to a Pt(II) center.[47,53] The $^{13}C\{^1H\}$ NMR spectrum of complex **9** lacks the resonance of the $C_{aryl}-Br$ moeity. Instead a new triplet resonance with platinum satellites is observed at $\delta$ 145.36 ppm with $^2J_{PC} = 18.5$ Hz and $^1J_{PtC} = 945$ Hz, indicating the presence of a $\sigma$-bound $Pt-C_{ipso}$ moeity coupled by two magnetically equivalent phosphorus atoms.[56] It is noteworthy that van Koten reported a series of stilbenoid-pincer complexes akin to complex **9** in which the chemical shift of the Pt(II) nucleus was affected by *para* substituents over 11 bonds.[57,58]

For complexes **1** and **2**, nearly identical five-spin $AMY_3$ systems flanked by six-spin $AMXY_3$ systems are observed by $^{19}F\{^1H\}$, $^{31}P\{^1H\}$, and $^{195}Pt\{^1H\}$ NMR spectroscopy (A, M = $^{31}P$, X = $^{195}Pt$ and Y = $^{19}F$). These NMR spectra were simulated with gNMR (version 5.0)[59] and were in very good agreement with the experimental data (Figure 1). Unusually large, long-range couplings between the $^{195}Pt$ and $^{19}F$ nuclei were observed with $^7J_{PtF} = 13.2$ Hz (**1**) and 11.8 Hz (**2**) (Table 1). The $^{19}F\{^1H\}$ NMR spectra show long-range $^{31}P-^{19}F$ spin coupling of ~3 Hz through eight bonds. The heteronuclear spin coupling is remarkable if one considers the distances. The estimated through-bond distances between the $^{195}Pt$ and $^{19}F$ nuclei are ~1.1 nm, and the distances between the $^{31}P$ and $^{19}F$ nuclei are ~1.3 nm. A homonuclear spin coupling over 11 bonds, $^{11}J_{FF} = 7.3$ Hz, with an internuclear distance of 1.4 nm, has been observed for a fully conjugated difluoropolyyne (Chart 1, **II**).[17]

For complexes **1** and **2**, no spectral changes were observed by varying: (i) the solvent polarity (acetone vs benzene), (ii) the concentration by a magnitude of order (2.8−28 mM), or (iii) the temperature (270 K vs 298 K). These experimental observations indicate that the long-range $^{195}Pt-^{19}F$ interactions involve through-bond rather than through-space spin−spin coupling, which is confirmed by X-ray analysis of complex **2** (Figure 2). Through space coupling can be observed if two nuclei are very close together and one of these nuclei has a nonbonding pair of electrons that can interact with the second nucleus.[60−63] However, in our case, the nuclei are too far apart.

Three-spin AMY systems flanked by four-spin AMXY systems are observed for complexes **3** and **4** by $^{19}F\{^1H\}$, $^{31}P\{^1H\}$, and $^{195}Pt\{^1H\}$ NMR spectroscopy (A, M = $^{31}P$, X = $^{195}Pt$, and Y = $^{19}F$). Calculated spectra are nearly identical with the experimental spectra, supporting the assigned spin system (Figure 3). The NMR spectra of complex **3** are temperature independent (270−298 K), whereas for complex **4** some broadening is observed at room temperature in the $^1H$ and $^{19}F\{^1H\}$ NMR spectra. As for complexes **1** and **2**, the spectral data of complexes **3** and **4** are also solvent (acetone-$d_6$ vs benzene-$d_6$) and concentration (2.8−28 mM, **3** and 6.5−30 mM, **4**) independent, suggesting through-bond spin−spin interactions. Large long-range coupling through six bonds between $^{195}Pt$ and $^{19}F$ is observed by both $^{195}Pt\{^1H\}$ and $^{19}F\{^1H\}$ NMR spectroscopy with $^6J_{PtF} = 11.6$ Hz. Furthermore, $^{31}P-^{19}F$ interactions with both $PEt_3$ ligands (*trans*-$^7J_{PF} = 3.5$ Hz and *cis*-$^7J_{PF} = 0.4$ Hz) were observed by $^{19}F\{^1H\}$ NMR spectroscopy. No $^{31}P-^{19}F$ spin interactions with the analogous nickel and palladium complexes were observed by us due to a relatively large line width in the $^{19}F\{^1H\}$ and $^{31}P\{^1H\}$ NMR spectra. For example, the singlet resonance of the aryl−F moiety of the nickel complex in acetone has a half line width, $\omega_{1/2}$, of ~6 Hz in the range 253−298 K. Measurements at lower temperatures were hampered due to solubility problems.

Colorless crystals of complexes **2** and **3** were obtained upon slow evaporation of THF−pentane solutions under a nitrogen atmosphere at room temperature. The X-ray analyses unambiguously confirm the spectroscopically observed $\eta^2$-coordination of the metal center to the carbon−carbon double bonds of ligands **6** and **7** (Figure 2). The $\pi$-backdonation from the electron-rich Pt center to the $\pi^*$ antibonding orbitals of the carbon−carbon double bond results in bond lengthening (i.e., C(7)−C(8) = 1.472(6) for **2** and 1.447(7) Å for **3**). For comparison, the length of the carbon−carbon double bond of *trans*-1,2-bis(4-pyridyl)ethylene is 1.333 Å.[54] Complexes **2** and **3** exhibit a nearly planar geometry around the metal center, which is in a plane containing a C=C moiety, and the

(51) Zenkina, O. V.; Karton, A.; Freeman, D.; Shimon, L. J. W.; Martin, J. M. L.; van der Boom, M. E. *Inorg. Chem.* **2008**, *47*, 5114.
(52) Zenkina, O. V.; Konstantinovski, L.; Freeman, D.; Shimon, L. J. W.; van der Boom, M. E. *Inorg. Chem.* **2008**, *47*, 3815.
(53) Still, B. M.; Kumar, P. G. A.; Aldrich-Wright, J. R.; Price, W. S. *Chem. Soc. Rev.* **2007**, *36*, 665.
(54) Asaro, F.; Lenarda, M.; Pellizer, G.; Storaro, L. *Spectrochim. Acta Part A* **2000**, *56A*, 2167.
(55) Lenarda, M.; Ganzerla, R.; Lisini, A.; Graziani, M.; Boschi, T. *Transition Met. Chem.* **1981**, *6*, 199.
(56) Terheijden, J.; van Koten, G.; Muller, F.; Grove, D. M.; Vrieze, K.; Nielsen, E.; Stam, C. H. *J. Organomet. Chem.* **1986**, *315*, 401.
(57) Batema, G. D.; Lutz, M.; Spek, A. L.; van Walree, C. A.; de Mello Donegá, C.; Meijerink, A.; Havenith, R. W. A.; Perez-Moreno, J.; Clays, K.; Büchel, M.; van Dijken, A.; Bryce, D. L.; van Klink, G. P. M.; van Koten, G. *Organometallics* **2008**, *27*, 1690.
(58) Batema, G. D.; van de Westelaken, K. T. L.; Guerra, J.; Lutz, M.; Spek, A. L.; van Walree, C. A.; de Mello Donegá, C.; Meijerink, A.; van Klink, G. P. M.; van Koten, G. *Eur. J. Inorg. Chem.* **2007**, 1422.
(59) Rummey, J. M.; Boyce, M. C. *J. Chem. Educ.* **2004**, *81*, 762.
(60) Patel, B. P.; Crabtree, R. H. *J. Am. Chem. Soc.* **1996**, *118*, 13105.
(61) Peris, E.; Lee, J. C.; Crabtree, R. H. *J. Chem. Soc., Chem. Commun.* **1994**, 2573.
(62) Mallory, F. B.; Luzik, E. D.; Mallory, C. W.; Carroll, P. J. *J. Org. Chem.* **1992**, *57*, 366.
(63) Barchi, J. J., Jr.; Jeong, L. S.; Siddiqui, M. A.; Marquez, V. E. *J. Biochem. Biophys. Methods* **1997**, *34*, 11.

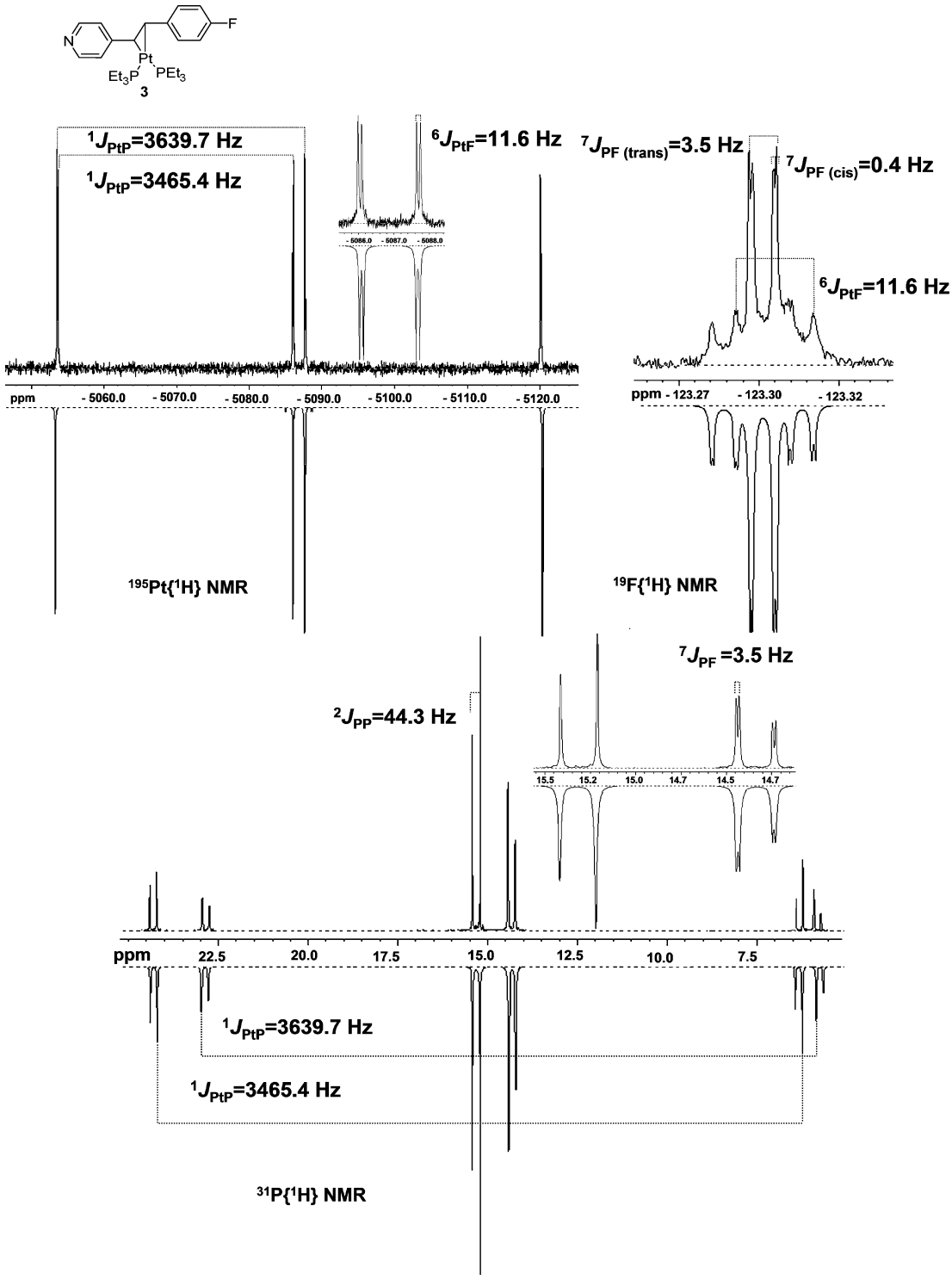


**Figure 3.** Experimental (upper) and simulated (lower) $^{31}P\{^1H\}$, $^{19}F\{^1H\}$, and $^{195}Pt\{^1H\}$ NMR spectra of complex **3** in acetone-$d_6$ showing the AMY spin system flanked with AMXY spin system (A, M = $^{31}P$, Y = $^{19}F$, and X = $^{195}Pt$). The simulated spectra were obtained with gNMR (version 5.0).[59]

two $PEt_3$ ligands with angles P(2)—Pt(1)—P(3) = 105.76(6)° (**2**) and 102.78(5)° (**3**), and C(7)—Pt(1)—C(8) = 40.47(17)° (**2**) and 40.00(19)° (**3**). These features are characteristic of Pt(0)−olefin complexes.[47,64,65] There is no common plane between the two aromatic rings. The arene carbon−carbon bond lengths are in the expected range of 1.332−1.412 Å (**2**) and 1.337−1.410 Å (**3**). For example, the arene carbon−carbon bond lengths of free ligand **6** are in the range of 1.324−1.391 Å.[66] The pyridyl and phenyl groups are twisted with respect to each other with angles of 28.61° (**2**) and 35.61° (**3**). Importantly, the intramolecular Pt···F distances, 7.08−7.66 Å (**2**) and 6.87 Å

(64) Collman, J. P.; Hegedus, L. S.; Norton, J. R.; Finke, R. G. *Principles and Applications of Organotransition Metal Chemistry*; University Science Books: New York, 1987.

(65) Astruc, D. *Organometallic Chemistry and Catalysis*; Springer: New York, 2007.

(66) Annoni, E.; Pizzotti, M.; Ugo, R.; Quici, S.; Morotti, R.; Casati, N.; Macchi, P. *Inorg. Chim. Acta* **2006**, *359*, 3029.

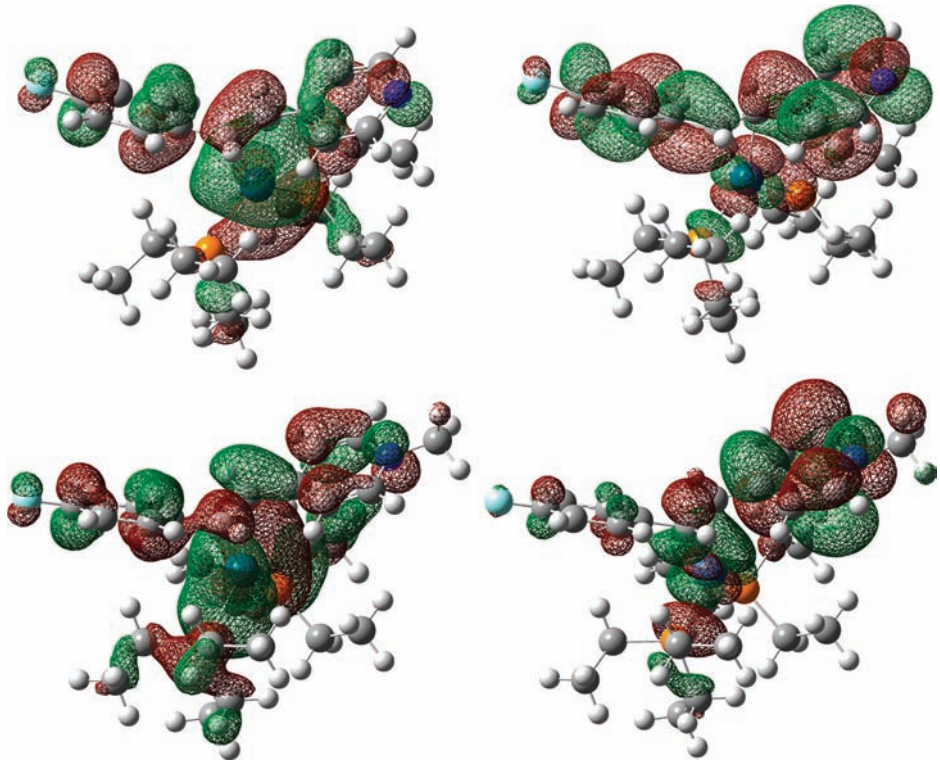

**Figure 4.** Calculated HOMO (left) and LUMO (right) of complexes **3** (top) and **4** (bottom) in benzene. Atomic color scheme: F - light blue, P - orange, Pt - teal, C - gray, H - white, N - dark blue.

(**3**), and intermolecular Pt···F distances, 5.79−7.31 Å (**2**) and 6.11 Å (**3**), are much larger than the sum of the van der Waals radii of F (1.47 Å) and Pt (1.75 Å).[23] Apparently, these distances are too large to permit any through-space coupling.

Complexes **3** and **4** were examined computationally using density functional theory (DFT) at the PBE0/SDD level of theory (see Experimental Section for full details). The calculated structure of **3** is in reasonable agreement with the obtained experimental X-ray crystallography structure (see Supporting information, Table S1). For example, the calculated C═C bond distance of 1.468 Å is close to the experimentally observed value of 1.447 Å. The Pt−C distances of 2.119 and 2.126 Å are similar to the values, 2.114 and 2.118 Å, measured by X-ray. Likewise, the 6.898 Å distance between the Pt and F atoms is very close to the distance, 6.877 Å, in the crystal, especially noting how far apart the two centers are. The HOMO and LUMO of complexes **3** and **4** in benzene as determined by DFT are presented in Figure 4. We noted the conjugation between the platinum, phosphorus, and fluorine centers, which is essential for through-bond spin coupling.[8−12]

If one compares the experimental NMR spectra of complexes **3** and **4** (see Supporting Information, Table S1), there are two major differences. First, the long-range $^{6}J_{PtF}$ coupling increases nearly 4-fold (11.6 versus 40.0 Hz). Second, in complex **4** the two olefinic carbons are substantially different. In both complexes, the bond lengths of the central C═C unit and of the fluorophenyl group are similar. However, upon methylation, the pyridinium ring acquires an alternating C−C, C═C, and C−N structure. The $^{1}$H NMR spectra show a shift of ∼1 ppm to $\delta$ 7.58 ppm for the ortho protons of the pyridinium group. Likewise, significant shifts are observed by $^{13}$C{$^{1}$H} NMR spectroscopy in the aromatic region. Furthermore, the exocyclic bond is considerably shorter (1.433 Å in **4** compared to 1.478 Å in **3**). This, in part, explains why the two olefinic carbons become different in the NMR spectra. As observed both in the X-ray and in the DFT calculations, quarternization of the pyridine moiety diminishes the size of the conjugated system. This in turn increases the conjugation in complex **4** between the platinum and fluorine centers and, thereby, increases the coupling constant between them. The relatively simple conjugation model presented here offers some insight in the long-range couplings. However, coupling constants depend on many variables.[5]

## Summary and Conclusions

Four new platinum complexes (**1**−**4**) have been identified that exhibit unusually large long-range $^{195}$Pt−$^{19}$F and $^{31}$P−$^{19}$F spin−spin interactions in solution (Table 1). These heteronuclear interactions are independent of temperature, solvent, and concentration, and this is indicative of through-bond spin−spin coupling. The X-ray-derived molecular structures of complexes **2** and **3** confirm the through-bond coupling as the large intra- and intermolecular distances (>5.7 Å) between the $^{19}$F and $^{195}$Pt or $^{31}$P nuclei rule out through-space interactions. The spin−spin couplings are readily observable regardless of the long internuclear distances (≥0.9 nm) between the metal center and the ligand. Apparently, the $\pi$-conjugated system of the stilbene (**5**) and stilbazole (**6**−**8**) ligands provides optimal conditions for spin−spin coupling between the NMR active nuclei, which is in agreement with

experimental[20] and theoretical studies.[5,17,67] Long-range $^6J_{FF}$ coupling in perfluorostyrenes was observed back in the 1960s.[68] Apparently, the interaction between the nuclei is hardly affected by the arylBr (**1**) or the pyridine (**2**, **3**) moieties. However, quaternization of the pyridine group of complex **3** resulted in a significant enhancement of the spin coupling between the platinum and fluorine atoms over six bonds by about half an order of magnitude ($^6J_{PtF} = 11.6$, **3** vs $^6J_{PtF} = 40.1$ Hz, **4**). The very good correlation between the simulated and experimental multinuclear NMR spectra of complexes **1**−**4** provides strong support for the presence of the five-spin $AMY_3$ (**1**, **2**) and three-spin AMY (**3**, **4**) systems flanked by the six-spin $AMXY_3$ (**1**, **2**) and four-spin AMXY (**3**, **4**) systems, respectively.[69] The straightforward preparation of these well-defined coordination complexes and the versatile molecular structure of stilbene, stilbazole, and related ligands may make these systems ideal for applications involving heteronuclear communication.

**Acknowledgment.** This research was supported by the Helen and Martin Kimmel Center for Molecular Design, the German−Israel Foundation (GIF), and the G. M. J. Schmidt Minerva Center.

**Supporting Information Available:** The Figure S1−S4, Table S1, crystallographic data (CIF) for complexes **2** and **3**, computed (DFT) Cartesian coordinates of complexes **3** and **4**, and a discussion on the complex coupling in the olefinic region of the $^{13}C\{^1H\}$ NMR spectra of complex **2**. This material is available free of charge via the Internet at http://pubs.acs.org.

IC801940H

(67) Barfield, M. *J. Chem. Phys.* **1968**, *48*, 4463.
(68) Callander, D. D.; Coe, P. L.; Matough, M. F. S.; Mooney, E. F.; Uff, A. J.; Winson, P. H. *Chem. Commun.* **1966**, *22*, 820.
(69) For an example of a heteronuclear spin system supported by simulation of NMR spectra, see: Fryzuk, M. D.; Haddad, T. S. *J. Am. Chem. Soc.* **1988**, *110*, 8263.